



HAL
open science

A murine model to study the gut bacteria parameters during complex antibiotics like cefotaxime and ceftriaxone treatment

Matthieu Grégoire, Florian Berteau, Ronan Bellouard, Quentin Lebastard, Philippe Aubert, Jacques Gonzales, François Javaudin, Anne Bessard, Pascale Bemer, Éric Batard, et al.

► To cite this version:

Matthieu Grégoire, Florian Berteau, Ronan Bellouard, Quentin Lebastard, Philippe Aubert, et al.. A murine model to study the gut bacteria parameters during complex antibiotics like cefotaxime and ceftriaxone treatment. Computational and Structural Biotechnology Journal, 2021, 19, pp.1423-1430. 10.1016/j.csbj.2021.02.019 . hal-03636869

HAL Id: hal-03636869

<https://hal.science/hal-03636869>

Submitted on 15 Mar 2023

HAL is a multi-disciplinary open access archive for the deposit and dissemination of scientific research documents, whether they are published or not. The documents may come from teaching and research institutions in France or abroad, or from public or private research centers.

L'archive ouverte pluridisciplinaire **HAL**, est destinée au dépôt et à la diffusion de documents scientifiques de niveau recherche, publiés ou non, émanant des établissements d'enseignement et de recherche français ou étrangers, des laboratoires publics ou privés.



Distributed under a Creative Commons Attribution - NonCommercial 4.0 International License

1 **Title: A murine model to study the gut bacteria parameters during complex antibiotics**
2 **like cefotaxime and ceftriaxone treatment.**

3

4 **Running title: Ceftriaxone increase intestinal carriage of ESBL-producing *Klebsiella***

5

6 Matthieu Grégoire^{1,2,#}, Florian Berteau², Ronan Bellouard^{1,2}, Quentin Lebastard^{2,3}, Philippe
7 Aubert⁴, Jacques Gonzales⁴, François Javaudin^{2,3}, Anne Bessard⁴, Pascale Bemer^{2,5}, Éric
8 Batard^{2,3}, Didier Lepelletier^{2,5}, Michel Neunlist⁴, Emmanuel Montassier^{2,3}, Éric Dailly^{1,2}

9

10 ¹Clinical Pharmacology Department, CHU Nantes, Nantes, France

11 ²EE1701, Microbiotas Hosts Antibiotics and bacterial Resistances, Nantes University, France

12 ³Emergency Department, CHU Nantes, Nantes, France

13 ⁴UMR Inserm 1235, The Enteric Nervous System in gut and brain disorders, Nantes
14 University, France.

15 ⁵Bacteriology and Infection Control Department, CHU Nantes, Nantes, France

16

17 Email addresses:

18 Matthieu Grégoire: matthieu.gregoire@chu-nantes.fr

19 Florian Berteau: yfenwel85@hotmail.fr

20 Ronan Bellouard: ronan.bellouard@chu-nantes.fr

21 Quentin Lebastard: quentin.lebastard@chu-nantes.fr

22 Philippe Aubert: philippe.aubert@univ-nantes.fr

23 Jacques Gonzales: jacques.gonzales@univ-nantes.fr

24 François Javaudin: francois.javaudin@chu-nantes.fr

25 Anne Bessard: anne.bessard@univ-nantes.fr
26 Pascale Bemer: pascale.bemer@chu-nantes.fr
27 Éric Batard: eric.batard@chu-nantes.fr
28 Didier Lepelletier: didier.lepelletier@chu-nantes.fr
29 Michel Neunlist: michel.neunlist@univ-nantes.fr
30 Emmanuel Montassier: emmanuel.montassier@chu-nantes.fr
31 Éric Dailly: eric.dailly@chu-nantes.fr
32
33 #Corresponding author at: Laboratoire de Pharmacologie clinique, Hôtel Dieu, 9 Quai
34 Moncoussu, 44093 Nantes Cedex, France. Fax: +33 2 40 08 40 12. E-mail address:
35 matthieu.gregoire@chu-nantes.fr (M. Grégoire).

36
37
38
39
40

41 **Abstract :**

42 Background: The globally increasing resistance due to extended-spectrum beta-lactamase
43 producing *Enterobacteriaceae* is a major concern. The objective of this work was to develop a
44 murine model to study the gut bacteria parameters during complex antibiotics like cefotaxime
45 and ceftriaxone treatment and to compare the fecal carriage of ESBL-producing
46 *Enterobacteriaceae*.
47 Methods: SWISS mice were treated either with ceftriaxone or with cefotaxime or with NaCl
48 0.9% as a control group from day 1 to day 5. We performed a gavage at day 4 with a
49 *Klebsiella pneumonia* CTX-M9. We collected stools and performed pharmacological

50 measurements, cultures and 16S rRNA gene amplification and sequencing during the 12 days
51 of the stool collection.

52 Results: Mice treated with ceftriaxone were more colonized than mice treated with cefotaxime
53 after gavage (p-value = 0.008; Kruskal-Wallis test). Ceftriaxone and cefotaxime were both
54 excreted in large quantity in gut lumen but they drove architecture of the gut microbiota in
55 different trajectories. Highest levels of colonization were associated with particular
56 microbiota composition using principal coordinate analysis (PCoA) which were more often
57 achieved in ceftriaxone-treated mice and which were preceded by highest fecal antibiotics
58 concentrations in both cefotaxime or ceftriaxone groups. Using LEfSe, we found that twelve
59 taxa were significantly different between cefotaxime and ceftriaxone-treated mice. Using
60 SplinctomeR, we found that relative abundances of *Klebsiella* were significantly higher in
61 CRO than in CTX-treated mice (p-value = 0.01).

62 Conclusion: Ceftriaxone selects a particular microbial community and its substitution of for
63 cefotaxime could prevent the selection of extended-spectrum beta-lactamase producing
64 *Enterobacteriaceae*.

65 **Keywords:** beta-lactamase, gastrointestinal microbiome, enterobacteriaceae, extended-
66 spectrum beta-lactamase

67 **Introduction**

68 The increasing global resistance of *Enterobacteriaceae* to beta-lactams is a major public
69 health concern for the years to come and led the World Health Organization to classify the
70 resistance of *Enterobacteriaceae* to third-generation cephalosporins (3GC) as a critical
71 priority for research and development of new antibiotics in February 2017 (1). The majority
72 of 3GC-resistant *Enterobacteriaceae* produces extended-spectrum beta-lactamase (ESBL)
73 which increases morbidity and mortality, length of stay and health costs (2,3).

74 The microbiota would be composed of 800 to 1000 species comprising more than
75 7000 different strains (4). Within this population of 10^{12} to 10^{13} individuals, bacteria are
76 carrying genes for antibiotic resistance. Antibiotics conduct to a partial destruction of the gut
77 bacteria (mainly anaerobic) susceptible to the given agent, thus leaving room and access to the
78 necessary resources for organisms resistant to this treatment (5). Knowing that gut microbiota
79 is a reservoir for ESBL-producing *Enterobacteriaceae*, their multiplication can lead to
80 excretion in the external environment and inter-individual transmission (6,7). These germs
81 may be responsible for infections that will be difficult to treat (8). One of the possibilities to
82 limit the emergence of resistant mutants is to choose the antibiotics that have the lowest
83 impact on the microbiota but knowledge that could drive this choice are still scarce.

84 Studies show that use of 3GC and exposure to 3GC favors ESBL-mediated resistance
85 in *Enterobacteriaceae* (9–11). Although they have similar antibacterial spectrum, ceftriaxone
86 (CRO) and cefotaxime (CTX) may have different impact on ESBL-mediated resistance.
87 Specifically, it is advocated that CRO has more impact on the gut microbiota than CTX, due
88 to higher biliary elimination than CTX (12). In a large multicentric study involving 701
89 health care facilities, use of CRO is positively associated with 3GC-resistant *E. coli*, whereas
90 CTX use is not (13). However, use of both 3GC is associated with 3GC-resistant *Klebsiella*
91 *pneumonia* (*Kp*) in the same study, and with 3GC-resistant *E. cloacae* in another one (12,13).

92 The impact of replacing CRO by CTX on resistance to 3GC is reported in 2 hospital-level
93 studies. In one center, it is associated with a slower growth of high-level cephalosporinase
94 mediated resistance, mainly in *E. cloacae*, but has no impact on ESBL-mediated resistance
95 (14). More recently, Tan *et al.* show that switching from CRO to CTX is associated with a
96 decreased incidence of hospital-acquired infection caused by ESBL-producing
97 *Enterobacteriaceae* (15). Lately, Burdet *et al.* do not found different effects on the microbiota
98 in healthy volunteers treated 3 days with CRO or CTX (16). Hence, the ecological advantage
99 of CTX on CRO remains debated, and no experimental study has compared the effects of
100 CRO and CTX on the fecal microbiota.

101 The main objective of this experimental work was to develop a murine model to study the gut
102 bacteria parameters during complex antibiotics like CTX and CRO treatment and to compare
103 the fecal carriage of ESBL-producing *Enterobacteriaceae*.

104

105

106 **Materials and Methods**

107 **Animals**

108 SWISS non-consanguineous albino mice provided by the JANVIER laboratory (Le Genest-
109 Saint-Isle, France) were used. These are robust and non-aggressive animals often used for
110 pharmacological modeling and already used to study the carriage of multidrug-resistant
111 *Enterobacteriaceae* (17). We used females aged 6 weeks and weighing between 25 and 30 g,
112 guaranteed without pathogens. The mice were housed at the Animal Research Center of the
113 Institute of Health Research 2, University of Nantes, in a controlled environment (day/night
114 cycle of 12h, extinction 7:30 pm) with a controlled sterile diet. After a review of the literature
115 on multidrug-resistant bacteria implantation in murine models, the number of mice per
116 treatment group was set at 15 (18–21). In addition, mice were isolated in individual cages to

117 prevent cross-contamination by coprophagia. Drinking water and food were provided *ad*
118 *libitum*. Study was approved by the French Ministry of Higher Education and Research
119 (APAFIS 8528, Site agreement A44279, ethics committee 006).

120

121 **Antibiotics**

122 Compared with CTX structure, CRO has a basic 2-(2-amino-4-thiazolyl)-2-(Z)-
123 methoxyimino-acetyl side chain which led to a very long elimination half-life of 8 hours in
124 human, high beta-lactamase stability and extremely high chemotherapeutic efficacy against a
125 broad spectrum of Gram-positive and Gram-negative pathogens. Therefore, in human, due to
126 its extended half-life, CRO is used one or twice daily while CTX is used 3-time daily or in
127 continuous infusion. Reconstitution of CRO and CTX was performed in physiological saline
128 (NaCl 0.9%) to obtain initial concentrations of 100 g/L. Mice were randomized in three
129 groups: Group 1 received CRO 250 mg/kg twice daily subcutaneously from day 1 to day 5,
130 group 2 received CTX 500 mg/kg three times daily from day 1 to day 5 and the control group
131 received NaCl 0.9% three times daily from day 1 to day 5. Taking into account the very short
132 half-life of these molecules in mice and the concentrations usually found in humans, it was
133 decided to use high dosages corresponding to 5 times the recommended dosage in humans
134 when treating severe infections such as bacterial meningitis or infectious endocarditis (22–
135 24). Indeed, we carried out a preliminary pharmacokinetic study to choose the optimal dosage
136 to be adopted based on the plasma and fecal concentrations usually found in patients treated
137 for infections. Maximum plasma concentration and mean plasma half-life of CTX (after 250
138 mg/kg, n = 5) in our mice were 207 mg/L and 24 minutes, respectively and maximum plasma
139 concentration and mean plasma half-life of CRO (after 500 mg/kg, n = 1) were 264 mg/L and
140 78 minutes, respectively. Plasma concentrations were similar to those usually observed in
141 human and concentrations of CRO and CTX in the feces were they similar to those observed

142 by previously published studies (279 µg/g and 167 µg/g respectively) (17,25,26). We
143 therefore chose to administer 500 mg/kg three times a day for CTX and 250 mg/kg twice a
144 day for CRO. All subcutaneous injections were 200 µL.

145

146 **Bacterial strain and gavage**

147 The strain used for gavage was a clinical isolate of *Kp*, carrying the beta-lactamase CTX-M9
148 (MIC of CTX: 512 mg/L, MIC of CRO: 2046 mg/L). The plasmids harboring most bla_{CTX-M}
149 are transferable among bacterial cells, especially in the gut (27). Inocula of 10⁵ CFU were
150 prepared immediately before gavage using a spectrophotometer. Gavage was done at day 4 of
151 the antibiotic treatment.

152 Three runs of 5 mice in each group (CRO, CTX and NaCl) were performed.

153

154 **Stool collection and culture**

155 Stool sampling was performed at day 1, 4, 6, 8, 10 and 12. On the day of sampling, each
156 mouse was placed in a clean cage for 1 hour to collect his stool and was returned to his
157 "accommodation" cage. Stools were immediately frozen at -80 ° C.

158 Each stool was weighed and then crushed (Ultraturrax Tube Drive®, IKA™,
159 Germany) with 10 µL saline per milligram of stool. Serial dilutions were performed in the
160 fresh state, then manual inoculations of 100 µL on chromogenic media with mixture of
161 antibiotics, including cefpodoxime (ChromID ESBL, BioMérieux™, Marcy L'Etoile, France)
162 were carried out before incubation at 37°C of 24h.

163 The detection threshold was $2 \log_{10}$ CFU/g stool. At least one colony per culture
164 medium was identified using mass spectrometry (MALDI TOF, Vitek MS®, Biomérieux™,
165 Marcy L'Etoile, France) to confirm genus and species.

166

167 **16S rRNA gene amplification and sequencing**

168 Fecal samples were kept frozen at -80°C until they were processed. After fecal DNA
169 isolation using the PowerSoil® DNA Isolation Kit (MoBio Laboratories, Carlsbad, CA fecal
170 DNA kit) including an enzymatically cell lysis step, amplicons spanning the variable region 4
171 of bacterial 16S rRNA gene were generated and sequenced using Illumina Mi-seq platform at
172 the University of Minnesota Genomic Center, Twin Cities, MN (28). The 16S rRNA gene
173 sequencing data from the Illumina runs were trimmed and filtered using SHI7 (29). We then
174 performed operational taxonomic units (OTUs) assignment using ‘NINJA-OPS’ against the
175 Greengenes 13.8 database as a reference, by clustering the sequences with a threshold of 97%
176 pairwise identity (30,31). Next, we used Quantitative Insights Into Microbial Ecology
177 (QIIME) 1.9.1 for diversity analyses (32). We presented beta diversity, based on Unweighted
178 UniFrac distances, a β -diversity measure that uses phylogenetic information to compare
179 samples, with principal coordinate analysis (PCoA), using the plugin
180 beta diversity through plots.py and a sampling depth of 17236 (33). We applied the
181 PERMANOVA method on the previously obtained dissimilarity matrices. PERMANOVA
182 was performed using 1000 permutations. We computed alpha diversity metrics using non-
183 phylogeny metrics (Observed OTUs, Chao1 index, Shannon index) with the plugin
184 alpha rarefaction.py and a sampling depth of 17236. We also performed Random Forest (RF)
185 classification with 500 trees and ten-fold cross-validation using the plugin
186 supervised_learning.py and the OTU table (34). To study longitudinal variation in our

187 samples, we used SplinectomeR, that applied smoothing splines to summarize data for
188 straightforward hypothesis testing in longitudinal studies (35).

189 To compare samples collected in CRO and CTX mice, we used the LEfSe tool on the
190 OTU table collapsed at genus level. LEfSe (Linear discriminant analysis Effect Size)
191 determines the features (here, taxa collapsed at genus level) most likely to explain differences
192 between classes by coupling standard tests for statistical significance with additional tests
193 encoding biological consistency and effect relevance (36). To identify significant associations
194 between microbial and phenotypic variables, we applied a linear multivariate regression
195 model specifically adapted to microbiome data: MaAsLin, Multivariate microbial Association
196 by Linear models (37). MaAsLin constructs boosted, additive general linear models to
197 associate metadata and transformed microbial taxonomic or functional relative abundances.
198 Since microbial community profiles are typically high dimensional, boosting is used for
199 feature selection over potential covariates to identify those most associated with each
200 microbial feature. Selected metadata are then used in a general linear model with metadata as
201 predictors and arcsin-square root transformed microbial relative abundances from the OTU
202 table collapsed at genus level as the responses. The dataset generated and analyzed during the
203 current study is available in the NCBI repository under the accession number PRJNA701545
204 (<http://www.ncbi.nlm.nih.gov/bioproject/701545>). The OTU table, collapsed at genus level is
205 also provided as **Table S1**. Compositional biplot that simultaneously displays the sample
206 clustering and phyla of the gut microbiomes of the fecal samples collected from CTX- and
207 CRO-treated mice are represented in **Fig. S1**.

208

209 **Pharmacokinetics**

210 Stools collected were weighed, diluted in 0.9% NaCl (10 mg/100 μ L) and homogenized by
211 grinding in ball tubes and sonication. The ground material obtained was centrifuged (5 min,
212 13000 g, + 4 ° C).

213 For the CTX and desacetyl-CTX assay, 125 μ L of the supernatant was mixed with 125
214 μ L of a methanol/ZnSO₄ 3M solution (80/20 v/v) and 250 μ L of an acetonitrile solution
215 containing the deuterated internal standard (¹³C₂, ²H₃-CTX). After centrifugation of the
216 mixture (10 min, 13000 g, +4°C), 2 μ L of the supernatant were injected into the
217 chromatographic system (H-Class® Acquity UPLC system, Waters™, St Quentin en
218 Yvelines, France). The system consisted of a Kinetex 2.6 μ m C18 column in a
219 thermostatically controlled oven at 50°C, mobile phases with a binary gradient
220 [(acetonitrile/formic acid 0.1% v/v) and (ultrapure water/formic acid 0.1% v/v)] at a flow rate
221 of 0.8 mL/min and a mass spectrometer monitoring of the m/z ratios (456, 460, 414) for
222 respectively CTX, ¹³C₂, ²H₃-CTX, and desacetyl-CTX for 4 min after each injection.

223 For the CRO assay, 250 μ L of the supernatant was mixed with 250 μ L of acetonitrile
224 solution containing the deuterated internal standard (¹³C, ²H₃-CRO). After centrifugation (5
225 min, 13000 g, + 4°C) of the mixture, 300 μ L of the supernatant were mixed with 2 ml of
226 dichloromethane. After centrifugation, 2 μ L of the supernatant was injected into the H-Class®
227 Acquity UPLC system. The chromatographic system consisted in a Kinetex 2.6 μ m C18
228 column in a furnace thermostatically controlled at 50°C, mobile phases with a binary gradient
229 (acetonitrile and a 1 mM aqueous ammonium acetate solution) at a flow rate of 0.8 mL/min
230 and a mass spectrometer monitoring of the m/z ratios (555, 559) for the CRO and ¹³C, ²H₃-
231 CRO respectively for 4 min after each injection. For both methods, reproducibility and
232 inaccuracy were less than 15%, the limit of quantification was 10 μ g/g stool for CRO, CTX
233 and desacetyl-CTX.

234

235 **Quantification and statistical analysis**

236 Statistical analyzes were performed using RStudio® (<https://www.r-project.org/>) and
237 GraphPad Prism® 6.0 (GraphPad Software Inc. TM, La Jolla CA, USA). Areas under the curve
238 (AUC) were calculated by trapezoidal method. Negative culture were fixed at 2 log₁₀ CFU/g
239 stool.

240 The Kruskal-Wallis test was used for unpaired data. The post hoc multiple comparison
241 tests were performed using the Dunn method. Non-parametric Mann-Whitney tests were
242 performed between the two-by-two groups with Bonferroni correction. All tests were defined
243 with alpha risk determined a priori as significant if ≤ 0.05 .

244

245 **Results**

246

247 **CRO induced higher ESBL-*Kp* colonization than CTX**

248 Results of growth culture are shown in **Figure 1A**. The absence of pre-existing 3GC-resistant
249 strains prior to gavage by ESBL-producing *Kp* is demonstrated by the negativity of stool
250 cultures on the day of gavage. CRO-induced ESBL-producing *Kp* colonization was
251 consistently higher than CTX-induced colonization from day 4 to day 12 (p-value = 0.008,
252 Mann-Whitney test) (**Figure 1B**).

253

254 **CRO and CTX are both excreted in gut lumen**

255 Detectable fecal concentrations for CRO were observed and were maintained until 10 days
256 after the end of treatment (**Figure 1C**). Detectable concentrations for CTX and its active
257 metabolite desacetyl-CTX were observed until 10 days after stopping treatment (**Figure 1D**).
258 Fecal exposures to antibiotics were assessed using the area under the curve (AUC) of fecal

259 concentrations over time. AUC of CTX and desacetyl-CTX were 1015 $\mu\text{g}\cdot\text{g}^{-1}\cdot\text{day}$ and 3962
260 $\mu\text{g}\cdot\text{g}^{-1}\cdot\text{day}$ respectively. AUC of CRO was 1859 $\mu\text{g}\cdot\text{g}^{-1}\cdot\text{day}$.

261

262

263 **CRO and CTX drive the architecture of the gut microbiota in different trajectories**

264 At baseline (i.e., before antibiotic treatment was started), we did not find any significant
265 difference between CTX, CRO-treated mice and control mice, in terms of alpha diversity
266 (ANOVA, Shannon index: p-value= 0.556, observed OTUs: p-value = 0.143). Overall, we
267 found a significant decrease in alpha diversity between antibiotic-treated mice and control
268 mice (ANOVA, Shannon index: p-value = 0.001, observed OTUs: p-value = 0.001,
269 chao1 index: p-value = 0.001). However, we did not find significant difference in alpha
270 diversity between CTX and CRO-treated mice (ANOVA, Shannon index: p-value = 0.665,
271 observed OTUs: p-value = 0.530, chao1 index: p-value = 0.855, **Fig. S2**). Importantly, alpha
272 diversity decreased significantly with time in both CTX and CRO-treated mice (p-value =
273 0.01), but this decrease was not different between CTX-treated mice and CRO-treated mice
274 (p-value = 0.50).

275 Using Unweighted UniFrac distances, at baseline (i.e., before antibiotic treatment was
276 started), we did not find any significant difference between we did not find any significant
277 difference between CTX, CRO-treated mice and control mice (PERMANOVA, $r^2 = 0.068$, p-
278 value = 0.492, **Figure S3A**). Overall, we found that both CTX and CRO significantly alter the
279 overall architecture of the gut microbiota when compared to control mice (PERMANOVA, r^2
280 = 0.128, p-value = 0.001, principal component 1: ANOVA, p-value < 0.001, principal
281 component 2: ANOVA, p-value < 0.001). Moreover, CRO and CTX drove the architecture of
282 the gut microbiota in 2 different trajectories (PERMANOVA, $r^2 = 0.142$, p-value = 0.001,

283 principal component 1: ANOVA, p-value = 0.358, principal component 2: ANOVA, p-value
284 = 0.002, **Figure S3A**).

285 We observed that the time after the antibiotic treatment had a strong impact on the
286 beta-diversity with higher Principal Coordinate (PC) 1 and PC2 scores observed at day 12
287 **(Fig. 2A)**. Before treatment and until day 4, CRO- and CTX-treated mice were similar and
288 differences appeared at day 8 and increased at day 12. A more important inter-individual
289 variability was observed in CTX-treated than in CRO-treated mice at day 12. Beta-diversity
290 trajectories by mouse are represented in **Fig. S3B**. Supervised learning using Random Forests,
291 a machine learning method using OTUs as predictive features, accurately assigned samples to
292 their source population (CTX or CRO-treated mice) based on taxonomic profiles at the OTU
293 level (83.3% accuracy, 3 times better than the baseline error rate for random guessing). Thus,
294 based on microbiome data only, we were able to predict if a mouse received CRO or CTX
295 treatment.

296 Using LEfSe on the OTU table collapsed at the genus level (36), we found that 12 taxa were
297 significantly different between CTX and CRO-treated mice. Specifically, CRO-treated mice
298 were associated with a significant gain in *Lactobacillus*, *Klebsiella*, unclassified
299 *Enterobacteriaceae*, and *Parabacteroides* when compared to CTX-treated mice, that were,
300 conversely, associated with increase in *Enterococcus*, unclassified *Carnobacteriaceae*,
301 unclassified *Planococcaceae*, *Granulicatella*, unclassified *Lactobacillales*, unclassified
302 *Enterococcaceae*, *Vagococcus* and *Anaeoplasma* (**Figure 2B**). The most significant
303 differentiating taxa between CTX and CRO-treated mice are represented in **Fig. S4A and B**.
304 Significantly different taxa between CRO and control mice and CTX and control mice
305 respectively are described in **Fig. S4C and 5D**. Comparison of antibiotic treated mice (all
306 collected samples in CTX and CRO-treated mice) and control mice (all collected samples) is
307 represented un **Table S3**.

308 To confirm these changes, we used SplinectomeR that enables group comparisons in
309 longitudinal microbiome studies. First, we plotted the longitudinal changes in the three groups
310 of mice, antibiotic-treated mice (CRO or CTX) and control mice. We found that in control
311 mice, gut microbiota composition was relatively stable along time, based on the OTU table
312 collapsed at genus level (Fig. S5A), whereas, gut microbiota composition was dramatically
313 altered following CRO and CTX treatment (**Fig. S5B and C**). We confirm that *Enterococcus*
314 was significantly higher in CTX than in CRO-treated mice along days of collection (p-
315 value=0.01, **Figure 2C**) and that *Klebsiella* was significantly higher in CRO than in CTX-
316 treated mice (p-value = 0.01, **Figure 2D**). Unclassified *Enterobacteriaceae*, *Parabacteroides*
317 and *Lactobacillus* were also higher in CRO than in CTX-treated mice (p-value = 0.04, p-value
318 = 0.03 and p-value = 0.1, respectively).

319

320 **Antibiotic fecal concentrations impact on OTU abundance**

321 We investigated the relationship between CRO, CTX and desacetyl-CTX fecal concentrations
322 and the gut microbiome by identifying significant multivariate linear associations using
323 MaAsLin. The relative abundance of 34 OTUs was positively correlated with CRO fecal
324 concentration levels, including members of *Sphingomonadaceae*, *Microbacteriaceae*,
325 *Sphingobacteriaceae* and *Enterobacteriaceae* families. Two OTUs were positively correlated
326 with CTX/desacetyl-CTX fecal concentration levels, corresponding to *Lactobacillus* and
327 *Leucobacter* genera.

328 We observed that higher antibiotic concentration levels were not associated with highest PC1
329 and PC2 scores but preceded these metagenomics alterations leading to colonization by
330 ESBL-producing *Kp*.

331

332 **ESBL-producing *Klebsiella pneumoniae* carriage is associated to taxonomic changes**

333 We observed that clustering of fecal samples was partly driven by the increased carriage of
334 ESBL-producing *Kp* ($r^2 = 0.0641$, p-value = 0.001, **Fig. S6**). Higher colonization levels being
335 associated with higher PC1 and PC2 scores in the two groups, i.e. with the most altered
336 microbiota. This beta-diversity pattern was mainly found in CRO-treated mice and especially
337 at day 12 as described in **Fig. S3B** and suggested that CRO selects a microbial community
338 which promotes colonization by ESBL-producing *Kp*. Conversely, highest inter-individual
339 diversity observed at day 12 in CTX-treated mice was associated with in a lower level of
340 colonization. We found that 8 taxa from the OTU table collapsed at genus level, were
341 significantly different between mice displaying a high level of ESBL-producing *Kp* and those
342 displaying a low level (**Fig. S6B**). Specifically, mice with a high level were associated with a
343 significant gain in *Klebsiella* and unclassified *Pseudomonadaceae* when compared to low
344 level mice, that were, conversely, associated with increase in unclassified *Bacteroidales*,
345 unclassified *Desulfovibrionaceae*, *Sutterella*, unclassified *Peptococcaceae*, unclassified
346 *Clostridiaceae* and *Akkermansia*.

347 These results were confirmed by a negative association found between intensity of
348 ESBL-producing *Kp* carriage and OTUs from *Bacteroidales* and *Clostridiaceae* (**Table S2**).

349

350 **Discussion**

351 This experimental study shows three main results: (i) CRO appears to promote higher fecal
352 carriage of ESBL-producing *Kp* than CTX; (ii) both antibacterial agents altered fecal
353 microbiotas, but CRO had a more important impact than CTX; (iii) higher level of fecal
354 colonization by ESBL-producing *Kp* was associated with more altered microbiota. These
355 results suggest that the effect of CRO on *Kp* colonization could be mediated by its effect on
356 the intestinal microbiota.

357 We observe that fecal *Kp* levels were significantly higher in CRO-treated mice than in 2 other
358 groups (CTX and NaCl) but were equivalent in control and CTX-treated mice. We cannot
359 explain these results neither by the fecal concentrations observed during the experience nor by
360 the MIC of the strain. Indeed, concentrations of CRO and CTX in the feces were they similar
361 to those observed by previously published studies (17,25,26). Moreover, we cannot stated that
362 MIC of CRO and CTX were different regarding the variability in measurement (38).
363 Therefore, we made 2 hypotheses: the first based on the modification of the architecture of the
364 microbiota and the second based on the mechanism of action of these 2 3GC.

365 Indeed, we found that CRO and CTX drove the architecture of the gut microbiota in 2
366 different trajectories. As expected, we found a significant decrease in alpha diversity between
367 antibiotic-treated mice and control mice but we did not find significant difference in alpha
368 diversity between CTX and CRO-treated mice (16). If before the treatment and until day 4, it
369 was impossible to tell the difference between CRO- and CTX-treated mice, differences
370 appeared at day 8 and were accentuated at day 12. A more important inter-individual
371 variability was observed in CTX-treated mice which do not reached all the maximum values
372 of PC1 and PC2 at day 12 contrary to CRO-treated mice which reached high PC1 and PC2
373 values. Interestingly, higher *Kp*-colonization levels were associated with more altered
374 microbiota in the two groups and higher antibiotic concentration levels were not associated
375 with highest PC1 and PC2 scores but were preceded by these metagenomics alterations.
376 Conversely, highest inter-individual diversity observed at day 12 in CTX-treated mice was
377 associated with a lower level of colonization. These data suggested that CRO could select a
378 microbial community which promotes colonization by ESBL-producing *Kp* more easily than
379 CTX. These modifications have not been observed by Burdet *et al.* but their work focused on
380 low dosages of CRO given over only 3 days and in healthy individuals which are not
381 comparable to those potentially given in more serious infections (16). The only 2 subjects

382 with changes in the microbiota were those with detectable CRO in the stool but previous
383 study that CRO is more frequently found in the stool in high concentrations and similar to that
384 which we find (16,26).

385 Our results challenge also the pharmacokinetic hypothesis considering that CRO only could
386 selected more ESBL-producing *Enterobacteriaceae* because of a higher fecal elimination than
387 CTX (12). As explain before, we observed detectable concentration of CRO, CTX and its
388 active metabolite desacetyl-CTX until 10 days after stopping treatment in faeces (39). These
389 results confirm those of Grall *et al.* who found digestive excretion of CTX in significant
390 proportions (17). We could also hypothesize that desacetyl-CTX plays a role in the prevention
391 of carriage ESBL-producing *Enterobacteriaceae*. Indeed, if the bactericidal activity of
392 desacetyl-CTX is generally considered to be lower than CTX (the MIC of desacetyl-CTX is
393 8-fold higher than that of CTX on susceptible strains of *Kp*), desacetyl-CTX could act as a
394 beta-lactamase inhibitor and could potentiate the action of CTX as suggested by previous
395 studies (40,41). To reinforce this hypothesis, Labia *et al* showed that desacetyl-CTX was
396 much more stable to hydrolysis by beta-lactamase than CTX and could have a sustained
397 bactericidal effect even in the presence of these enzymes (42).

398 These data are crucial for the comprehension of the parameters influencing the carriage of
399 ESBL-producing *Enterobacteriaceae*, especially for patient displaying a high risk of
400 colonization such as patient treated with antibiotics or travelers in endemic area.

401 Our study has several limitations. First, we used 16S rRNA sequencing that limits
402 taxonomic identification at genus level. Therefore, we were not able to identify species or
403 strains that differ between CRO and CTX treated. In addition, our work is limited to a single
404 strain of ESBL-producing *Enterobacteriaceae* and deserves to be strengthened by testing
405 other strains.

406

407 **Conclusions**

408 In mice, both CRO and CTX modify the microbiota but CRO promotes more the carriage of a
409 strain of ESBL-producing *Kp*. If CRO appears to select a favorable specific microbial
410 community for the installation of this bacteria in a concentration-dependent way, CTX and
411 particularly its active metabolite desacetyl-CTX could prevent colonization because of a beta-
412 lactamase inhibitor effect.

413

414 **Acknowledgments**

415 This work was funded by the association AGISMED TOXICOLOGIE.

416

417 **Authors' contributions**

418 M.G., E.M. and E.D. designed the experiments, M.G., F.B., R.B. conducted animal
419 experiments, M.G., F.B., R.B., F.J. and P.B. conducted bacterial culture, MG., P.A., A.B. and
420 J.G. conducted functional exploration experiments, Q.L. and E.M. performed metagenomics
421 analysis, F.B., R.B. and E.D. conducted pharmacokinetics measurements, M.G., F.B., E.M,
422 E.D., E.B, D.L. and M.N. wrote the manuscript and created figures.

423

424 **Ethics approval and consent to participate**

425 Ethics approval was not required for the study.

426

427 **Competing interests**

428 The authors declare no competing interests.

429

430 **References**

- 431 1. WHO-PPL-Short_Summary_25Feb-ET_NM_WHO.pdf [Internet]. [cited 2018 Aug 30].
432 Available from: [http://www.who.int/medicines/publications/WHO-PPL-](http://www.who.int/medicines/publications/WHO-PPL-Short_Summary_25Feb-ET_NM_WHO.pdf)
433 [Short_Summary_25Feb-ET_NM_WHO.pdf](http://www.who.int/medicines/publications/WHO-PPL-Short_Summary_25Feb-ET_NM_WHO.pdf)
- 434 2. Pitout JDD, Laupland KB. Extended-spectrum beta-lactamase-producing
435 Enterobacteriaceae: an emerging public-health concern. *Lancet Infect Dis*. 2008
436 Mar;8(3):159–66.

- 437 3. de Kraker MEA, Wolkewitz M, Davey PG, Koller W, Berger J, Nagler J, et al. Burden
438 of antimicrobial resistance in European hospitals: excess mortality and length of hospital
439 stay associated with bloodstream infections due to *Escherichia coli* resistant to third-
440 generation cephalosporins. *J Antimicrob Chemother.* 2011 Feb;66(2):398–407.
- 441 4. Bäckhed F, Ley RE, Sonnenburg JL, Peterson DA, Gordon JI. Host-bacterial mutualism
442 in the human intestine. *Science.* 2005 Mar 25;307(5717):1915–20.
- 443 5. Ruppé E, Andremont A. Causes, consequences, and perspectives in the variations of
444 intestinal density of colonization of multidrug-resistant enterobacteria. *Front Microbiol.*
445 2013;4:129.
- 446 6. Donskey CJ. The role of the intestinal tract as a reservoir and source for transmission of
447 nosocomial pathogens. *Clin Infect Dis Off Publ Infect Dis Soc Am.* 2004 Jul
448 15;39(2):219–26.
- 449 7. Lerner A, Adler A, Abu-Hanna J, Cohen Percia S, Kazma Matalon M, Carmeli Y.
450 Spread of KPC-producing carbapenem-resistant Enterobacteriaceae: the importance of
451 super-spreaders and rectal KPC concentration. *Clin Microbiol Infect Off Publ Eur Soc*
452 *Clin Microbiol Infect Dis.* 2015 May;21(5):470.e1-7.
- 453 8. Razazi K, Mekontso Dessap A, Carteaux G, Jansen C, Decousser J-W, de Prost N, et al.
454 Frequency, associated factors and outcome of multi-drug-resistant intensive care unit-
455 acquired pneumonia among patients colonized with extended-spectrum β -lactamase-
456 producing Enterobacteriaceae. *Ann Intensive Care.* 2017 Dec;7(1):61.
- 457 9. Colodner R, Rock W, Chazan B, Keller N, Guy N, Sakran W, et al. Risk factors for the
458 development of extended-spectrum beta-lactamase-producing bacteria in
459 nonhospitalized patients. *Eur J Clin Microbiol Infect Dis Off Publ Eur Soc Clin*
460 *Microbiol.* 2004 Mar;23(3):163–7.
- 461 10. Kaier K, Frank U, Hagist C, Conrad A, Meyer E. The impact of antimicrobial drug
462 consumption and alcohol-based hand rub use on the emergence and spread of extended-
463 spectrum beta-lactamase-producing strains: a time-series analysis. *J Antimicrob*
464 *Chemother.* 2009 Mar;63(3):609–14.
- 465 11. Lee J, Pai H, Kim YK, Kim NH, Eun BW, Kang HJ, et al. Control of extended-spectrum
466 beta-lactamase-producing *Escherichia coli* and *Klebsiella pneumoniae* in a children's
467 hospital by changing antimicrobial agent usage policy. *J Antimicrob Chemother.* 2007
468 Sep;60(3):629–37.
- 469 12. Muller A, Lopez-Lozano JM, Bertrand X, Talon D. Relationship between ceftriaxone
470 use and resistance to third-generation cephalosporins among clinical strains of
471 *Enterobacter cloacae*. *J Antimicrob Chemother.* 2004 Jul;54(1):173–7.
- 472 13. Gbaguidi-Haore H, Dumartin C, L'Hériteau F, Péfau M, Hocquet D, Rogues A-M, et al.
473 Antibiotics involved in the occurrence of antibiotic-resistant bacteria: a nationwide
474 multilevel study suggests differences within antibiotic classes. *J Antimicrob Chemother.*
475 2013 Feb;68(2):461–70.

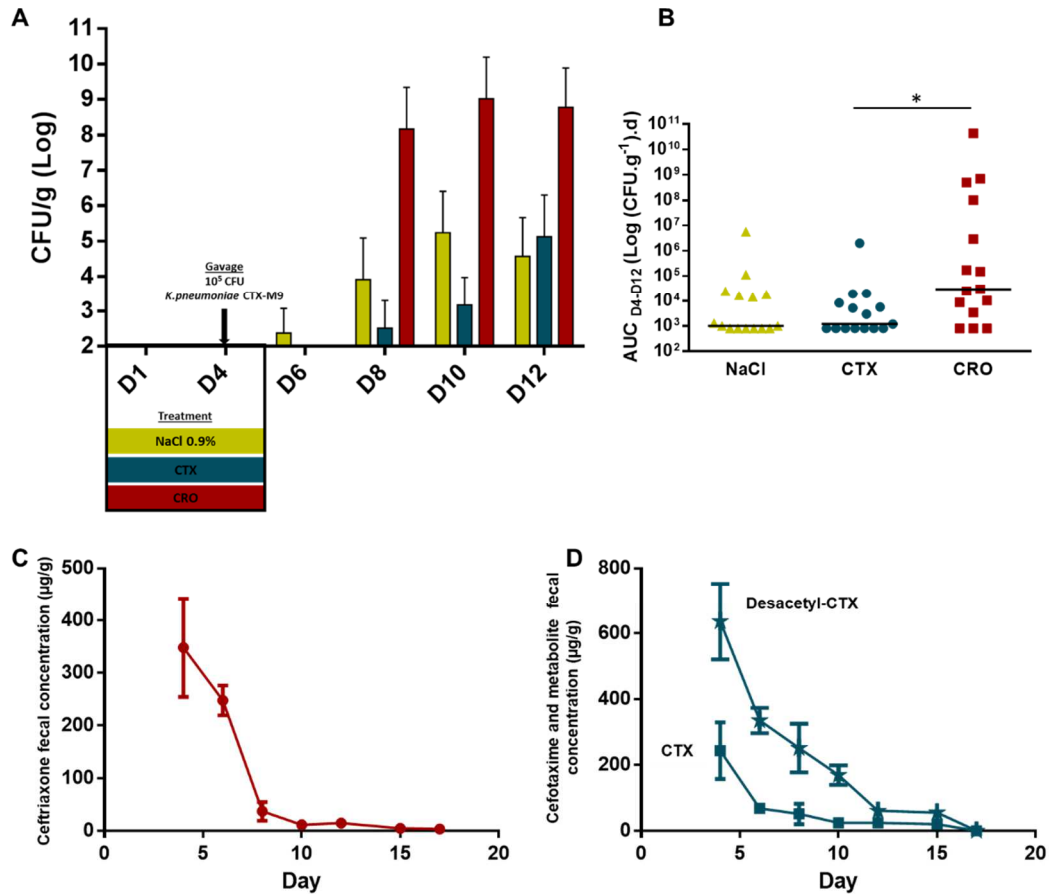
- 476 14. Grohs P, Kerneis S, Sabatier B, Lavollay M, Carbonnelle E, Rostane H, et al. Fighting
477 the spread of AmpC-hyperproducing Enterobacteriaceae: beneficial effect of replacing
478 ceftriaxone with cefotaxime. *J Antimicrob Chemother.* 2014 Mar;69(3):786–9.
- 479 15. Tan BK, Vivier E, Bouziad KA, Zahar J-R, Pommier C, Parmeland L, et al. A hospital-
480 wide intervention replacing ceftriaxone with cefotaxime to reduce rate of healthcare-
481 associated infections caused by extended-spectrum β -lactamase-producing
482 Enterobacteriaceae in the intensive care unit. *Intensive Care Med.* 2018;44(5):672–3.
- 483 16. Burdet C, Grall N, Linard M, Bridier-Nahmias A, Benhayoun M, Bourabha K, et al.
484 Ceftriaxone and Cefotaxime Have Similar Effects on the Intestinal Microbiota in Human
485 Volunteers Treated by Standard-Dose Regimens. *Antimicrob Agents Chemother.*
486 2019;63(6).
- 487 17. Grall N, Massias L, Nguyen TT, Sayah-Jeanne S, Ducrot N, Chachaty E, et al. Oral
488 DAV131, a charcoal-based adsorbent, inhibits intestinal colonization by β -lactam-
489 resistant *Klebsiella pneumoniae* in cefotaxime-treated mice. *Antimicrob Agents*
490 *Chemother.* 2013 Nov;57(11):5423–5.
- 491 18. Hoyen CK, Pultz NJ, Paterson DL, Aron DC, Donskey CJ. Effect of parenteral antibiotic
492 administration on establishment of intestinal colonization in mice by *Klebsiella*
493 *pneumoniae* strains producing extended-spectrum beta-lactamases. *Antimicrob Agents*
494 *Chemother.* 2003 Nov;47(11):3610–2.
- 495 19. Stiefel U, Pultz NJ, Donskey CJ. Effect of carbapenem administration on establishment
496 of intestinal colonization by vancomycin-resistant enterococci and *Klebsiella*
497 *pneumoniae* in mice. *Antimicrob Agents Chemother.* 2007 Jan;51(1):372–5.
- 498 20. Pultz MJ, Donskey CJ. Effects of imipenem-cilastatin, ertapenem, piperacillin-
499 tazobactam, and ceftriaxone treatments on persistence of intestinal colonization by
500 extended-spectrum-beta-lactamase-producing *Klebsiella pneumoniae* strains in mice.
501 *Antimicrob Agents Chemother.* 2007 Aug;51(8):3044–5.
- 502 21. Hertz FB, Løbner-Olesen A, Frimodt-Møller N. Antibiotic selection of *Escherichia coli*
503 sequence type 131 in a mouse intestinal colonization model. *Antimicrob Agents*
504 *Chemother.* 2014;58(10):6139–44.
- 505 22. Habib G, Lancellotti P, Antunes MJ, Bongiorni MG, Casalta J-P, Del Zotti F, et al. 2015
506 ESC Guidelines for the management of infective endocarditis: The Task Force for the
507 Management of Infective Endocarditis of the European Society of Cardiology (ESC).
508 Endorsed by: European Association for Cardio-Thoracic Surgery (EACTS), the
509 European Association of Nuclear Medicine (EANM). *Eur Heart J.* 2015 Nov
510 21;36(44):3075–128.
- 511 23. Tunkel AR, Hasbun R, Bhimraj A, Byers K, Kaplan SL, Scheld WM, et al. 2017
512 Infectious Diseases Society of America’s Clinical Practice Guidelines for Healthcare-
513 Associated Ventriculitis and Meningitis. *Clin Infect Dis.* 2017 Mar 15;64(6):e34–65.
- 514 24. van de Beek D, Cabellos C, Dzupova O, Esposito S, Klein M, Kloek AT, et al. ESCMID
515 guideline: diagnosis and treatment of acute bacterial meningitis. *Clin Microbiol Infect*
516 *Off Publ Eur Soc Clin Microbiol Infect Dis.* 2016 May;22 Suppl 3:S37–62.

- 517 25. Léonard F, Andremont A, Leclercq B, Labia R, Tancrede C. Use of beta-lactamase-
518 producing anaerobes to prevent ceftriaxone from degrading intestinal resistance to
519 colonization. *J Infect Dis.* 1989 Aug;160(2):274–80.
- 520 26. Arvidsson A, Leijd B, Nord CE, Angelin B. Interindividual variability in biliary
521 excretion of ceftriaxone: effects on biliary lipid metabolism and on intestinal microflora.
522 *Eur J Clin Invest.* 1988;18(3):261–6.
- 523 27. Ueda S, Ngan BTK, Huong BTM, Hirai I, Tuyen LD, Yamamoto Y. Limited
524 Transmission of blaCTX-M-9-Type-Positive *Escherichia coli* between Humans and
525 Poultry in Vietnam. *Antimicrob Agents Chemother.* 2015 Jun;59(6):3574–7.
- 526 28. Gohl DM, Vangay P, Garbe J, MacLean A, Hauge A, Becker A, et al. Systematic
527 improvement of amplicon marker gene methods for increased accuracy in microbiome
528 studies. *Nat Biotechnol.* 2016;34(9):942–9.
- 529 29. Al-Ghalith GA, Hillmann B, Ang K, Shields-Cutler R, Knights D. SHI7 Is a Self-
530 Learning Pipeline for Multipurpose Short-Read DNA Quality Control. *mSystems.* 2018
531 Jun;3(3).
- 532 30. Al-Ghalith GA, Montassier E, Ward HN, Knights D. NINJA-OPS: Fast Accurate Marker
533 Gene Alignment Using Concatenated Ribosomes. *PLoS Comput Biol.* 2016
534 Jan;12(1):e1004658.
- 535 31. DeSantis TZ, Hugenholtz P, Larsen N, Rojas M, Brodie EL, Keller K, et al. Greengenes,
536 a chimera-checked 16S rRNA gene database and workbench compatible with ARB.
537 *Appl Environ Microbiol.* 2006 Jul;72(7):5069–72.
- 538 32. Caporaso JG, Kuczynski J, Stombaugh J, Bittinger K, Bushman FD, Costello EK, et al.
539 QIIME allows analysis of high-throughput community sequencing data. *Nat Methods.*
540 2010 May;7(5):335–6.
- 541 33. Lozupone C, Lladser ME, Knights D, Stombaugh J, Knight R. UniFrac: an effective
542 distance metric for microbial community comparison. *ISME J.* 2011 Feb;5(2):169–72.
- 543 34. Knights D, Costello EK, Knight R. Supervised classification of human microbiota.
544 *FEMS Microbiol Rev.* 2011 Mar;35(2):343–59.
- 545 35. Shields-Cutler RR, Al-Ghalith GA, Yassour M, Knights D. SplinctomeR Enables
546 Group Comparisons in Longitudinal Microbiome Studies. *Front Microbiol.* 2018;9:785.
- 547 36. Segata N, Izard J, Waldron L, Gevers D, Miropolsky L, Garrett WS, et al. Metagenomic
548 biomarker discovery and explanation. *Genome Biol.* 2011 Jun 24;12(6):R60.
- 549 37. Morgan XC, Tickle TL, Sokol H, Gevers D, Devaney KL, Ward DV, et al. Dysfunction
550 of the intestinal microbiome in inflammatory bowel disease and treatment. *Genome Biol.*
551 2012 Apr 16;13(9):R79.
- 552 38. Mouton JW, Meletiadis J, Voss A, Turnidge J. Variation of MIC measurements: the
553 contribution of strain and laboratory variability to measurement precision. *J Antimicrob*
554 *Chemother.* 2018 Sep 1;73(9):2374–9.

- 555 39. Limbert M, Seibert G, Schrunner E. The cooperation of cefotaxime and desacetyl-
556 cefotaxime with respect to antibacterial activity and beta-lactamase stability. *Infection*.
557 1982;10(2):97–100.
- 558 40. Chin NX, Neu HC. Cefotaxime and desacetylcefotaxime: an example of advantageous
559 antimicrobial metabolism. *Diagn Microbiol Infect Dis*. 1984 Jun;2(3 Suppl):21S-31S.
- 560 41. Marone P, Navarra A, Monzillo V, Traverso A. Antibacterial activity of combined
561 cefotaxime and desacetyl-cefotaxime against aerobic and anaerobic gram-negative
562 bacilli. *Drugs Exp Clin Res*. 1990;16(12):629–33.
- 563 42. Labia R, Morand A, Kazmierczak A. The action of beta-lactamases on desacetyl-
564 cefotaxime and cefotaxime. *J Antimicrob Chemother*. 1984 Sep;14 Suppl B:45–51.
- 565

566 **Figure**

567

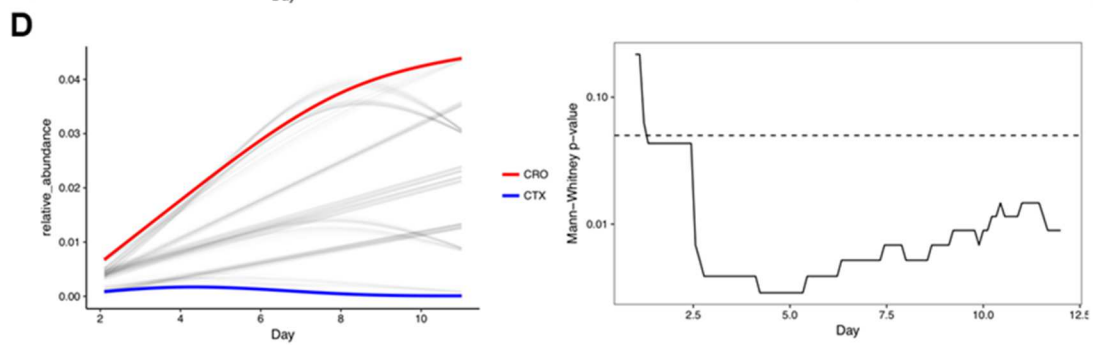
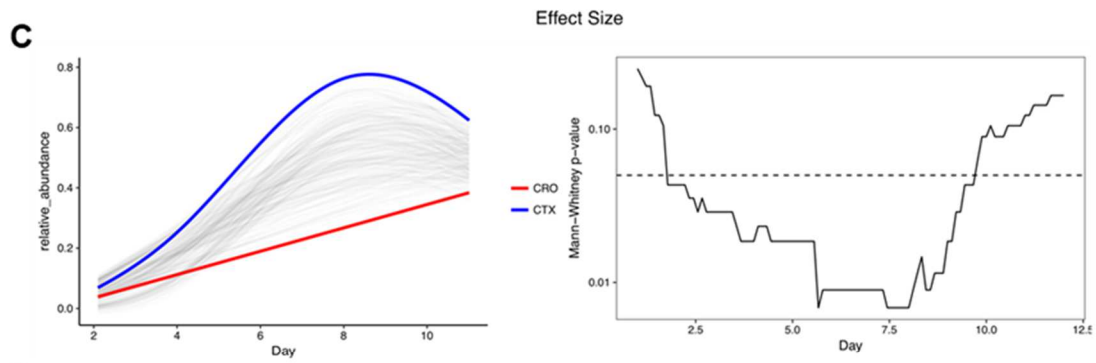
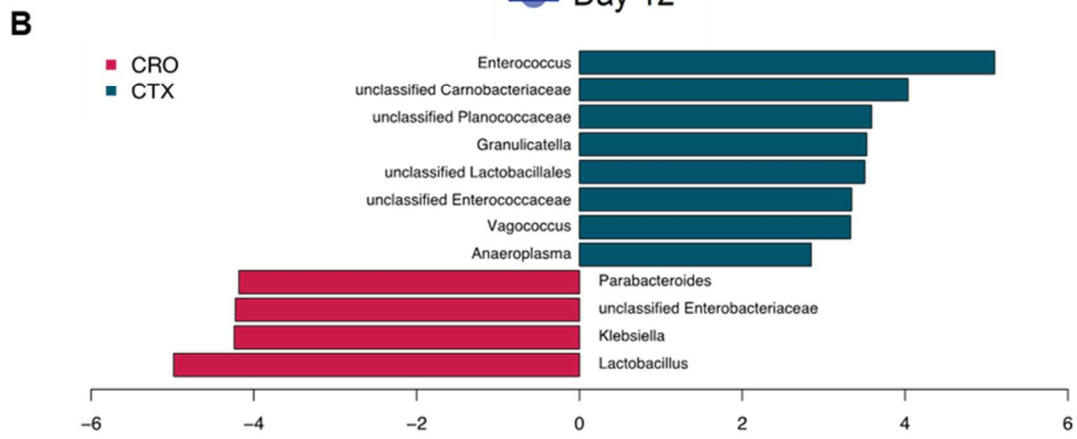
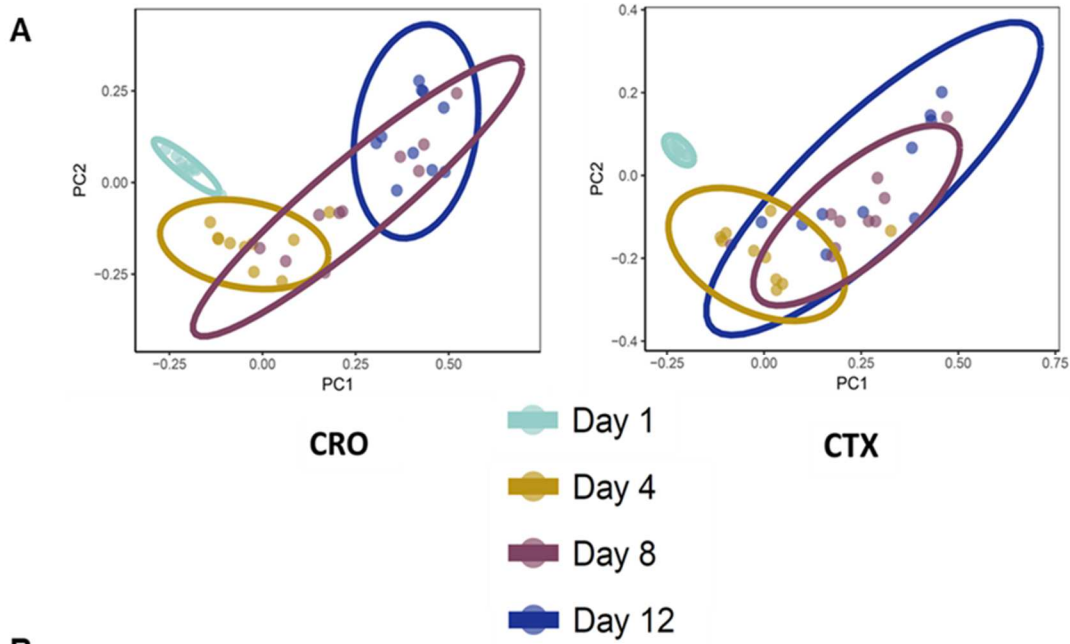


568

569 **Figure 1: Gut colonization by *Klebsiella pneumoniae*, transit modifications and fecal**
570 **concentrations of CRO and CTX**

571 (A) Quantification of fecal excretion of ESBL-producing *Kp* over time according to treatment
572 administered (n = 15 per group). The bars represent the mean and the range. (B)
573 Quantification of fecal excretion of ESBL-producing *Kp* over time according to treatment
574 administered (n = 15 per group). Lines correspond to loess-smoothed conditional means and
575 shading to SE. (C) Area under the curve (AUC) of ESBL-producing *Kp* excretion of control,
576 CTX and CRO groups. A statistically significant difference in colonization between CRO and
577 CTX was observed from day 4 to day 12 (p-value = 0.0078, Mann-Whitney test) and is

578 symbolized by an asterisk. (D) CRO fecal concentrations. (E) CTX (squares) and desacetyl-
579 CTX (stars) fecal concentrations. Values were indicated as mean +/- SEM (n = 10 per group).
580 Detection threshold was 10 µg/g.
581



583 **Figure 2: CRO and CTX alter the overall architecture of gut microbiota and induce**
584 **taxonomic changes**

585 (A) Beta diversity comparisons of the gut microbiomes of the fecal samples collected from
586 CTX- and CRO-treated mice. Beta diversity is represented by ellipse clustering according to
587 the day after the start of antibiotic treatment.

588 (B) Summary of the taxa that differentiate CTX from CRO-treated mice using Linear
589 discriminant analysis Effect Size analysis (LEfSe). At genus level, 12 taxa were significantly
590 different CTX from CRO-treated mice (absolute LDA log₁₀ score >2).

591 (C) Longitudinal changes in *Enterococcus* compared between CTX and CRO-treated mice,
592 using SplinectomeR with permuted spline test. (Left) *Enterococcus* relative abundance over
593 time distinguishes CTX (group spline in blue) and CRO-treated mice (group spline in red; 999
594 permutations, p-value = 0.01). Permuted splines represented in grey. The permuted splines lie
595 predominantly between the two observed curves, supporting the conclusion that this
596 difference is larger than expected by chance. (Right) The plot output of the sliding spliner
597 function shows the p-value at each specified interval derived from the distribution of points
598 from individuals' smoothed splines Dotted line indicates p-value = 0.05.

599 (D) Longitudinal changes in *Klebsiella* compared between CTX and CRO-treated mice, using
600 SplinectomeR with permuted spline test. (Left) *Klebsiella* relative abundance over time
601 distinguishes CTX (group spline in blue) and CRO-treated mice (group spline in red; 999
602 permutations, p-value = 0.01). Permuted splines represented in grey. The permuted splines lie
603 predominantly between the two observed curves, supporting the conclusion that this
604 difference is larger than expected by chance (Right) The plot output of the sliding spliner
605 function shows the p-value at each specified interval derived from the distribution of points
606 from individuals' smoothed splines. Dotted line indicates p-value = 0.05.

